ELSEVIER

Biophysical Chemistry 134 (2008) 1–9

Biophysical Chemistry

http://www.elsevier.com/locate/biophyschem

Physicochemical studies on goat pulmonary surfactant

Suvasree Mukherjee [a], Kajari Maiti [a], Mauricia Fritzen-Garcia [b], S.C. Bhattacharya [a], K. Nag [b], A.K. Panda [c,*], S.P. Moulik [a]

[a] *Centre for Surface Science, Department of Chemistry, Jadavpur University, Kolkata - 700 032, W. B., India*
[b] *Department of Biochemistry, Memorial University of Newfoundland, St. John's, Newfoundland, Canada*
[c] *Department of Chemistry, University of North Bengal, Darjeeling - 734 013, W.B., India*

Received 26 September 2007; received in revised form 4 December 2007; accepted 4 December 2007
Available online 15 December 2007

Abstract

The large aggregate (LA) fraction of goat pulmonary surfactant (GPS) was isolated and characterized. Goat lung surfactant extract (GLSE) was obtained by chloroform–methanol extraction of the saline suspended LA fraction. Total phospholipid (PL), cholesterol (CHOL), and protein were biochemically estimated. It was composed of ~83% (w/w) PL, ~0.6% (w/w) CHOL and ~16% (w/w) protein. CHOL content was found to be lower while the protein content was found to be higher than other mammalian pulmonary surfactants. Electrospray Ionization Mass Spectrometry (ESIMS) of GLSE confirmed dipalmitoylphosphatidylcholine (DPPC) as the major phospholipid species, with significant amounts of palmitoyl-oleoyl phosphatidylcholine (POPC), palmitoyl-myristoyl phosphatidylcholine (PMPC) and dioleoylphosphatidylcholine (DOPC). Functionality of the solvent spread GLSE film was carried out in a Langmuir surface balance by way of surface pressure (π)–area (A) measurements. A high value of π (~65 mN m^{-1}) could be attained with a lift-off area of ~1.2 nm^2 $molecule^{-1}$. A relatively large hysteresis was observed during compression–expansion cycles. Monolayer deposits at different π, transferred onto freshly cleaved mica by Langmuir–Blodgett (LB) technique, were imaged by atomic force microscopy. DPPC-enriched domains (evident from height analyses) showed dimensions of 2.5 μm and underwent changes in shapes after 30 mN m^{-1}. Functionality and structure of the surfactant films were proposed to be controlled by the relative abundances of protein and cholesterol.

Keywords: Pulmonary surfactant; Phospholipid; Cholesterol; Protein; Surface pressure; Domains; Electrospray Ionization Mass Spectrometry; Langmuir–Blodgett; Atomic force microscopy

1. Introduction

The study of pulmonary surfactant systems has significance in physiology, pathophysiology, biochemistry and physical chemistry. It also has a special importance in the field of life science [1]. Since its discovery by Pattle [2] and Clements [3], this complex system of surface active molecules in the mammalian lung, has provided an intriguing area for research. The pulmonary surfactant (PS) is essential for normal lung function. It reduces surface tension at the lung–air interface by way of forming a thin lining of surfactant films and thereby can attain near zero surface tension values (~72 mN m^{-1} surface pressure) at end expiration. Thus, PS can reduce the work of breathing [4–10]. As PS can reduce surface tension to near zero value, it can also prevent alveolar collapse. Besides this, it prevents alveolar edema and also has an important role in lung defense [11–13]. Much of research effort has been motivated by the finding that deficiency in PS is a primary cause of the respiratory distress syndrome (RDS) of premature infants [12,14–15]. According to recent findings, PS inactivation is an important secondary factor in adult respiratory distress syndrome (ARDS) that arises due to a variety of reasons.

PS is a complex mixture of lipids and proteins. Although some variations exist from species to species, the general composition of mammalian pulmonary surfactant is very similar. It is composed of ~85% PL, and a small amount of surfactant proteins (~10%) [5,7,16]. DPPC is the major saturated PL

* Corresponding author. Tel.: +91 9433347210; fax: +91 353269901.
E-mail address: akpanda1@yahoo.com (A.K. Panda).

0301-4622/$ - see front matter © 2007 Elsevier B.V. All rights reserved.
doi:10.1016/j.bpc.2007.12.002

(35–50%), which is primarily responsible for reducing the surface tension at the lung–air interface [17–19]. Others include unsaturated phosphatidylcholine (~25–35%) and acidic phospatidylglycerol (PG, 8–15%). The PLs present in trace amounts include phosphatidylinositol, phosphatidylethanolamine, phosphatidylserine [7,10]. There are four types of surfactant associated proteins (SP) of which SP-A and SP-D are hydrophilic proteins while SP-B and SP-C are hydrophobic in nature. According to Putz et al. [20], the biophysical activity of lung surfactant depends, to a large extent, on the presence of hydrophobic proteins SP-B and SP-C; these proteins enhance the formation of the surfactant film at the air–water interface, and thereby promote rapid lowering of surface tension upon film compression [21–26]. Surfactant proteins can also bind with carbohydrates and lipids to function as antimicrobial agents against a range of viruses, bacteria, fungi, etc. SP-A deficient animals are susceptible to lung infections but do not develop respiratory failure.

Because of general similarity in PS composition among mammals, organic solvent extracts of PS could easily be used as exogenous formulations in preventing RDS and ARDS to significant extents. Clinical formulations like Survanta™, Exosurf™, BLES™ (Bovine Lipid Extract Surfactant), etc., are well established formulations in the Western countries [27–28]. In India, the infant mortality rate due to RDS is high (two hundred thousand babies annually) [29]. The easy availability of goat lungs in India has motivated us to extract the surfactants from the lung of the slaughtered goats (in the local market) and study their surface physicochemical behaviors. Alternately, it could be overtly stated that current marketed artificial surfactants are not available in India, due to financial and cultural reasons. And it is this unavailability that results in the enormous death toll from NRDS. Thus, goat lung surfactants could represent a useful material for the manufacture of an artificial surfactant as an alternative to current products used in the Western world. With this objective, we have studied the physicochemical features of GLSE at the air–water interface in the Langmuir balance.

The rapid adsorption of PS to the air-alveolar surface to form surface active films is essential for maintaining normal lung function. DPPC, the main PS component possesses a bilayer gel of liquid crystal transition temperature at 41 °C and the cylindrical shape [30–31] of DPPC molecule enhanced its ability to sustain high surface pressure at physiological temperature. The generally accepted mechanism by which lung surfactant operates proposes that during expiration, different lipids and proteins phase separate within the PS film and certain components are removed or "squeezed-out" as the surface pressure is raised (or surface tension is reduced). The components may be lost from the surface temporarily and readsorbed during inspiration when surface pressure decreases. It has been suggested that a repeated compression–expansion cycle during breathing could result in monolayers highly enriched in DPPC, through squeeze-out of the more fluid non-DPPC lipids [21,32–33]. The presence of a surface monolayer highly enriched in DPPC is consistent with the properties of the lung [34]. A common feature of almost all lung surfactant and model mixtures is co-existence between a semi-crystalline solid/liquid-condensed phase (LC) in the monolayer, and a disordered fluid/liquid-expanded phase (LE) especially at higher surface pressure. The co-existence is important for surface mechanical properties of the film, which promotes high collapse pressure [35]. The most direct way to study the monolayer behavior of PS is to study them by way of surface pressure (π)–area (A) measurements. The Langmuir balance measures the change in surface pressure with the compression or expansion of the film. Two dimensional phase transitions can be realized by way of studying the monolayer behavior at the air–water interface.

The Atomic force microscopy (AFM) technique has been found to be a useful tool in studying the surface morphology [36–37]. A PS film, transferred onto an atomically flat substrate (freshly cleaved mica) by Langmuir–Blodgett technique can easily be studied by AFM. It is established that at higher surface pressures, LC regions are formed by way of accumulation of DPPC in the form of "domains" [38]. A DPPC-enriched domain has a typical height difference of ~1.2 nm with its surrounding fluid regions [39]. The dimension and morphology of a surface film structure can also be studied by AFM.

In the present study, biochemical assays of large aggregate (LA) fraction of goat lung surfactant were performed for phospholipids, protein and cholesterol. Film functionality was measured in terms of π–A isotherms in surface balance. Structures of the films by LB technique, transferred onto freshly cleaved mica, were studied at different surface pressures using AFM.

2. Materials and methods

2.1. Materials

Na_2CO_3, NaCl, $CaCl_2$, $(NH_4)_6Mo_7O_{24}$, KH_2PO_4, H_2SO_4, $HClO_4$ and NH_4OH were products from Merck, India. NaOH, sodium potassium tartrate, ascorbic acid, cholesterol and Foling–Ciocalteau reagent were purchased from SRL, India. Acetic anhydride from Fischer Chemic Ltd, Germany whereas DPPC and bovine serum albumin (BSA) from Sigma Chemicals, USA were used. Cholesterol was recrystallized from ethanol and all other chemicals were of analytical reagent grade and were used as received. HPLC grade $CHCl_3$ and CH_3OH were used in the study. Doubly distilled water with a specific resistivity of ~18 MΩ cm^{-1} was used in all preparations.

2.2. Methods

2.2.1. GPS isolation

Fresh goat lungs were obtained from a local butcher shop. Surfactant was isolated from the lungs within 4 h of tissue procurement. Lungs were lavaged with 0.15 M NaCl and 1.5 mM $CaCl_2$ solution (isotonic saline solution), and the return was collected by passive drainage. The lavage fluid was spun in a centrifuge (Heraeus Instruments, Model type, Biofuge 28RS, Germany). The initial spin was at low speed (360 g × 10 min) in order to remove tracheal debris and red blood cells in the pellet. The supernatant was subsequently spun at high speed (14,500 g × 30 min) to sediment a pellet of surfactant. The supernatant was discarded. The pellets, known

as large aggregate (LA) fraction, were resuspended in 1–2 ml of saline solution and were stored at −20 °C. It is to be noted here that normally the total lavage of the mammalian lung, after the removal of red blood cells and debris, needs to be spun at higher speed (40,000 g × 15) [40]. We have been restricted to relatively lower speed, which was compensated for by the increase in time.

2.2.2. Preparation of surfactant extract

The surfactant was extracted from the saline solution by the method of Bligh and Dyer [41]. For each 1 ml of saline solution of the surfactant, 3.5 ml 1:2 (v/v) $CHCl_3$:CH_3OH was added, and vortexed well. Then 1.25 ml of $CHCl_3$ and 1.25 ml H_2O were added and the mixture was thoroughly vortexed. It was spun again in a centrifuge at 1000 rpm for 5 min at room temperature to produce a two-phase system. The bottom organic phase (chloroform layer) was carefully withdrawn by pipette, and chloroform was removed by vacuum evaporator to finally obtain the lipid film. It was then redissolved in appropriate amount of 3:1 (v/v) $CHCl_3$:CH_3OH for monolayer studies.

2.2.3. Biochemical analysis

Biochemical assay of the goat lung extract was performed to determine its phospholipid, protein and total cholesterol contents. The phospholipid was estimated by an acid digestion method, in which, the lipids were digested to biphosphates by concentrated $HClO_4$ [42]. The released inorganic phosphate reacted with $(NH_4)_6Mo_7O_{24}$ and ascorbic acid to give a strong blue colour, and it was spectrophotometrically estimated by comparing with known standard KH_2PO_4 solution at 814 nm. The total cholesterol content in the surfactant extract was also spectrophotometrically estimated at 629 nm, when a green colour was produced by the interaction of $(CH_3CO)_2O$ and concentrated H_2SO_4 with cholesterol in chloroform solution [43]. The protein in the LA fraction was measured spectrophotometrically at 750 nm by the method of Lowry and coworkers using BSA as standard [44–45]. All measurements were performed for three different batches of goat lung surfactant extract at 25 °C, and the average of the three was used for analysis. Each batch comprised the lavage of two pairs of goat lungs. The wt.% compositions of the three batches are exemplified in the histogram depiction in Fig. 1. The results of the three batches were consistent. We do believe that to have a better idea on the composition–functionality–structure relationship, one must analyze two hydrophobic surfactant proteins SP-B and SP-C. Because these two proteins get extracted alongwith the lipids, which play crucial role in surfactant functionality. But because of limitations in facilities, we could only measure the total protein. The isolation and characterization of these two surfactant proteins could be done in the future.

Electrospray Ionization Mass Spectrometry (ESIMS) of GLSE was performed on a quadrupole mass spectrometer (model LC-MSD-Trap SL, Canada). Samples were injected by direct infusion with a syringe pump (model 22, Harvard Apparatus, SL, QC). The flow rate was fixed at 5.0 μL min^{-1}. LA fraction of PS, suspended in saline solution, was mixed with dymyristoylphosphatidylcholine (DMPC) and dymyristoylphosphatidylglycerol (DMPG). These two non-mammalian phospholipids were used as the internal standard. The suspension was then solvent extracted by Bligh and Dyer method [41]. Lipid extract was then redissolved in 25 μL of methanol:chlororform: water:NH_4OH (7:2:0.8:0.2, v/v) for run. The solution was then injected into the mass spectrometer, resulting the formation of singly charged $[M+H]^+$ and $[M-H]^-$ ions. Phosphatidylcholine species were detected by positive ionization, while PG and PI were detected using negative ionization [46]. The ion spray voltage was +4750 V for positive ion mode and −4500 V for negative ion mode. Dry heated nitrogen gas was used as the carrier gas. For each spectrum a minimum of 50 scans were averaged with a dwell time of 10 ms per data point. PL molecular species were identified by comparing the *m*/*z* of the various peaks with the calculated formula weight of compounds and from the literature values of identified animal species [47]. Intensity of individual species was corrected to mass units using the formula weights to obtain a relative mass ratio of individual molecular species [48].

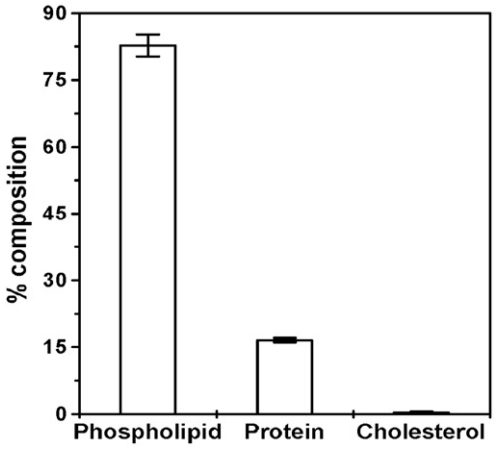

Fig. 1. Biochemical compositions of the large aggregate fraction of goat pulmonary surfactant. An average of three samples was taken in the calculation. In each batch two lung pairs were used.

2.2.4. π–A measurements

Surface pressure (π)–area (*A*) measurements were performed in a Langmuir balance (Model: 2004C, Apex Instruments Co., India). The trough has an initial area of 15 × 25 cm^2. Solvent spread films of GLSE were prepared using a 1.0 mg/ml solution. The solvent was composed of a mixture of 3:1 v/v $CHCl_3$:CH_3OH mixture. The required amount of GLSE solution was spread onto the air–water interface using a 25 μL Hamilton microsyringe. The subphase used was 0.15 M NaCl and 1.5 mM $CaCl_2$ solution (saline solution). A 15 min time was allowed for the evaporation of the solvent and in attaining uniformity of the monomolecular film. It was then compressed slowly with a barrier speed of 5 mm min^{-1}. In another set of experiment, both compression and expansion of the surface film were performed with a barrier speed of 50 mm min^{-1}. In this experiment higher amount of GLSE was spread to have a higher initial surface pressure (~10 mN m^{-1}). Five such cycles on the film were studied in order to understand the reversibility pattern of the surfactant film, an essential criterion of the respiratory performance of the lung.

2.2.5. AFM measurements

PS monolayers were transferred onto a substrate of freshly cleaved mica by LB transfer technique. The substrates were pre-immersed in the subphase. After the desired surface pressure was attained, a wait period of 5 min was provided for the equilibration of the film. An upstroke of 1 cm min^{-1} was tendered to the substrate whereby the monolayer was deposited onto the substrate. The fall in surface pressure during the monolayer transfer was compensated for, by automated compression of the barrier. After the LB deposit was obtained, it was stuck onto a stainless steel disk with double sided adhesive tape. Samples were imaged within an hour of deposition, with a Nanoscope III AFM (Digital Instruments, CA, USA). Images were taken using a J scanner by contact mode. A silicon nitride tip with a force constant of 0.12 N m^{-1} was used for scanning. After images were obtained, they were flattened and analyzed to get the size and height profiles.

All the experiments were carried out at 25±0.1 °C.

3. Results and discussion

3.1. Biochemical assay

LA fraction of GPS was analyzed to estimate the PL, CHOL and protein contents. All the bioassays were performed using three different batches of PS, and were then averaged. Results are graphically presented in Fig. 1. The average PL, CHOL and protein contents of six pairs of goat lungs were found to be 40, 0.3, and 8 mg respectively. (Approximate body weight of one animal was 15 kg). In terms of relative composition, it was found that the LA fraction of goat PS constituted 82.8, 16.6 and 0.6% (w/w) PL, protein and CHOL respectively. Relative abundances of PL, CHOL and protein contents of GPS have been compared in Table 1 with results of other species. It is known that normally mammalian PS is composed of ~85 wt.% PL, ~10 wt.% protein and remaining part is composed of different neutral lipids, including cholesterol [7], although there could be biological variations from species to species, as shown in Table 1. Our present set of results was found to be comparable with the literature values only in terms of the PL composition. Interestingly, CHOL content was found to be lower while higher protein content was found in the present study.

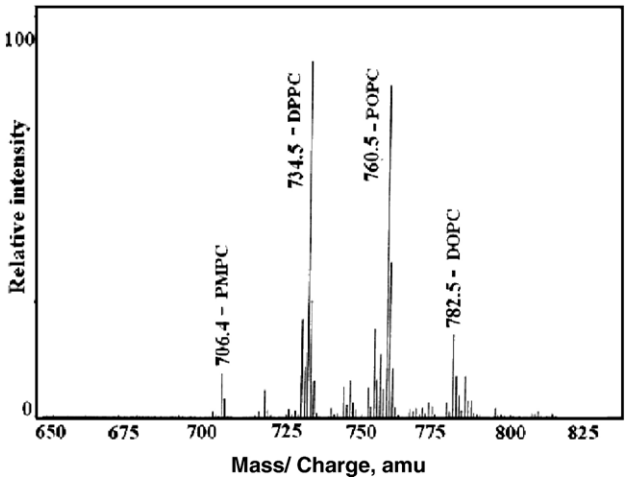

Fig. 2. ESIMS spectra of the major phosphocholine (PC) species present in GLSE. Expanded diagram between 650 and 850 Da is illustrated.

The expanded ESIMS spectra between 700 and 800 Da are presented in Fig. 2. The peaks correspond to molecular weights of PMPC [M+1=706.5], DPPC [M+1=734.57], POPC [M+1=760.5], and 1-steroyl, 2-linoleoyl (SLPC)+DOPC [M+1=786.6]. The latter two species, SLPC and DOPC are not distinguishable by mass spectrometry. It should be noted that ESIMS analysis as conducted here did not identify, which fatty acids are at the 1- and 2-position. The results have shown that DPPC constituted about 40% of the phosphatidylcholines, and was the major component of GLSE. POPC, DOPC, PMPC, the mono and di-unsaturated species were also present in significant amounts, 36, 8 and 4% respectively, in the phospholipid pool. Comparative charts have been made in Table 2 with the PC composition of other mammalian PS. In this table only the mostly abundant PC species are mentioned. The results were quite consistent with previous reports, except for POPC, which was present in a larger amount [48].

3.2. π–A isotherms

The surface pressure (π)–area (*A*) measurements performed on the monomolecular films of GLSE, are depicted in Fig. 3. It may be mentioned that based on the composition of GLSE, its average molecular weight was found to be 720, taking into

Table 1
Comparison of various parameters of surfactant composition between goat and other mammalian species

Species	Composition (wt.%)		
	Phospholipid	Cholesterol	Protein
Goat	82.8	0.6	16.6
Cow [10]	87.0	3.0	10.0
Sheep [7,56]	85.8	6.7	7.5
Ringed seal [56]	87.1	12.5	0.4
California sea lion [56]	81.4	7.6	11.0
Northern elephant seals [56]	81.3	2.4	16.3
Rat [40]	74.8	6.4	18.8
Rabbit [7,56]	80.0	–	–
Human [7,56]	80.5	7.3	12.2

Table 2
Comparison of various phosphatidylcholine molecular species of surfactant between goat and other species

Species	Phosphatidylcholine molecular species (mol%)			
	16:0/14:0	16:0/16:0	16:0/18:1	18:0/18:2
				18:1/18:1
Goat	4.0	40.0	36.0	8.0
Cow [48]	7.3	37	25.4	2.8
Pig [57]	8.8	47.2	15.5	–
Rabbit [58]	8.0	35	20	20
Rat [58]	9.0	42	8	10
Human [58]	10.0	55	13	8

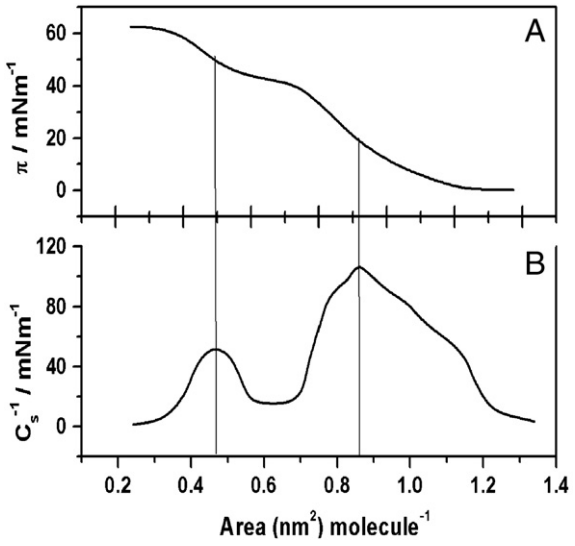

Fig. 3. (A) Surface pressure (π)–area (A) isotherms of solvent spread GLSE monomolecular films at the air–water interface at 25 °C. (B) Variation of compression modulus of the film with molecular area.

account of all the PL components as well as SP-B and SP-C. Surface pressure began rising at an area per molecule (A) of ~1.2 nm^2 molecule^{-1}. This value of A called the lift-off area or limiting area, was in conformity with other mammalian surfactants [49]. BLES, porcine, rat and calf lung surfactants also showed lift-off area at ~1.2 nm^2 molecule^{-1}. For lipid extract fraction of PS, the basic composition is almost the same, except in our case with a higher POPC content (that change contributed a little to the average molar mass of GLSE). Therefore, the lift-off area could be expected to be the same as other mentioned systems. At π~45 mN m^{-1}, a plateau was observed. Such a plateau region is not uncommon. Porcine, bovine and other mammalian surfactants produced similar regions [50–51]. In our earlier studies with rat [40] and BLES [48], we observed the appearance of such a plateau at ~42 mN m^{-1}. This phenomenon is thought to indicate "squeezing-out" of some active ingredients of GLSE into the subphase. Thereafter, π showed a steady increase that leveled off at 60 mN m^{-1}. After the squeezing-out phenomenon was over, the remaining lipids performed at the interface to increase π, until the surface film manifested collapse at 65 mN m^{-1}. Above given explanation needs experimental verification. Because of large trough volume (1.5 L) such estimation was not practicable in this study.

Phase transitions in the surface films were also examined in terms of isothermal film compressibility (C_S), given by the following relation

$$C_S = -(1/A)(\partial A/\partial \pi)_T. \quad (1)$$

The reciprocal of compressibility i.e. C_S^{-1}, (called compression modulus) is another way of demonstrating the transitions. Both modes of representations are depicted in Fig. 3A and B. Two transitions marked with vertical lines in the figures were witnessed. The first and second transitions corresponded to peaks of 100 and 45 mN m^{-1} at 0.86 and 0.47 nm^2 molecule^{-1} respectively. With increased compression, the expanded, fluid or disordered surface film suffered an appreciable transition, which subsequently produced a smaller transition due to restrictions in the molecular packing at the interface.

In order to study the reversibility of the surfactant films, as already mentioned earlier, greater amounts of surfactant were spread over the subphase. Compression–expansion isotherms for five consecutive cycles were measured as depicted in Fig. 4. Significant hysteresis was observed in the initial cycles, which was greatly reduced by the fifth cycle. The first cycle produced a large hysteresis and the plateau region seen between 60 and 40% trough areas was reduced and shifted to 25–30% area on the expansion limb of the curve. This is likely to reflect an appreciable loss in material from the interface to the bulk. Subsequent cycles evidenced continuous hysteresis with decreasing efficiency with downward shifts of cycle heights (63 to 48 mN m^{-1}). The material lost, with all probability, were fluid lipids like POPC. The lower cholesterol content could be another reason for the observation. Further studies are required for a better understanding. It is known that unsaturated PLs are generally unable to sustain high surface pressures, and are pushed out of the interface towards a reservoir of material underneath the film [28,52–53].

3.3. AFM studies

Solvent spread films of GLSE were transferred onto freshly cleaved mica surface at different surface pressures using LB techniques. They were then subsequently scanned in the contact mode in the AFM in air. It may be mentioned that for soft substances, usually tapping mode of imaging is used. But for the PS films it is established that deformity in the image structures does not occur even in the contact mode of imaging. Further, the surface heterogeneity can be better envisaged in the contact mode. Therefore several scans were performed on our samples, and then they were suitably processed using the offline software. Images were found to be reproducible within the frame of biological variations. Representative images at different surface pressures are

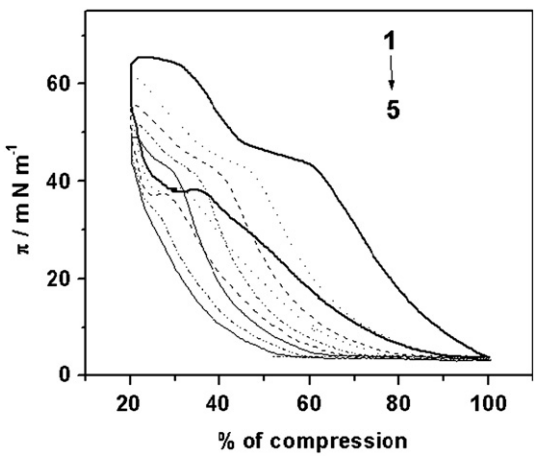

Fig. 4. Compression–expansion cycles for the GLSE solvent spread films at 25 °C. Sufficient amount of surfactant was spread at the air–water interface to have an initial surface pressure ~3–4 mN m^{-1}. 5 cycles are illustrated in the diagram.

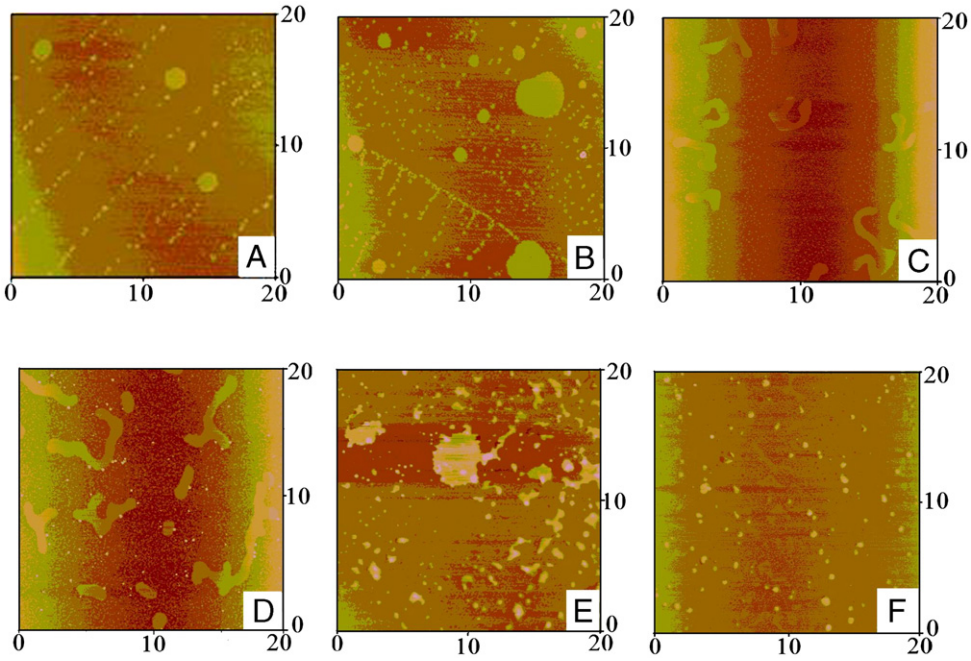

Fig. 5. Atomic force microscopic images of GLSE solvent spread films transferred onto freshly cleaved mica surface at different surface pressures (mN m^{-1}). A, 10; B, 20; C, 30; D, 40; E, 50 and F, 60. Scan area (μm^2): 20×20.

shown in Fig. 5. The present results were different from earlier findings on other mammalian pulmonary surfactants as well as of some model systems. Circular shaped domains resulted at surface pressures <20 mN m^{-1}, above which domain shapes changed drastically. Dimensions of the circular domains were of the order of 2–4 μm, smaller than other systems, like bovine, rat, porcine lung surfactants or model surfactant systems [49–50]. For this reason the morphology of the surface structure could not be seen at the air–water interface using epifluorescence microscopy (which has much lower resolution than AFM). Above π=20 mN m^{-1}, elongated noodle shaped domains appeared in the surface film which increased in size and length up to 40 mN m^{-1}; at a few units above 50 mN m^{-1} uneven surface morphologies of smaller dimensions with no characteristic organizations were noticed. These

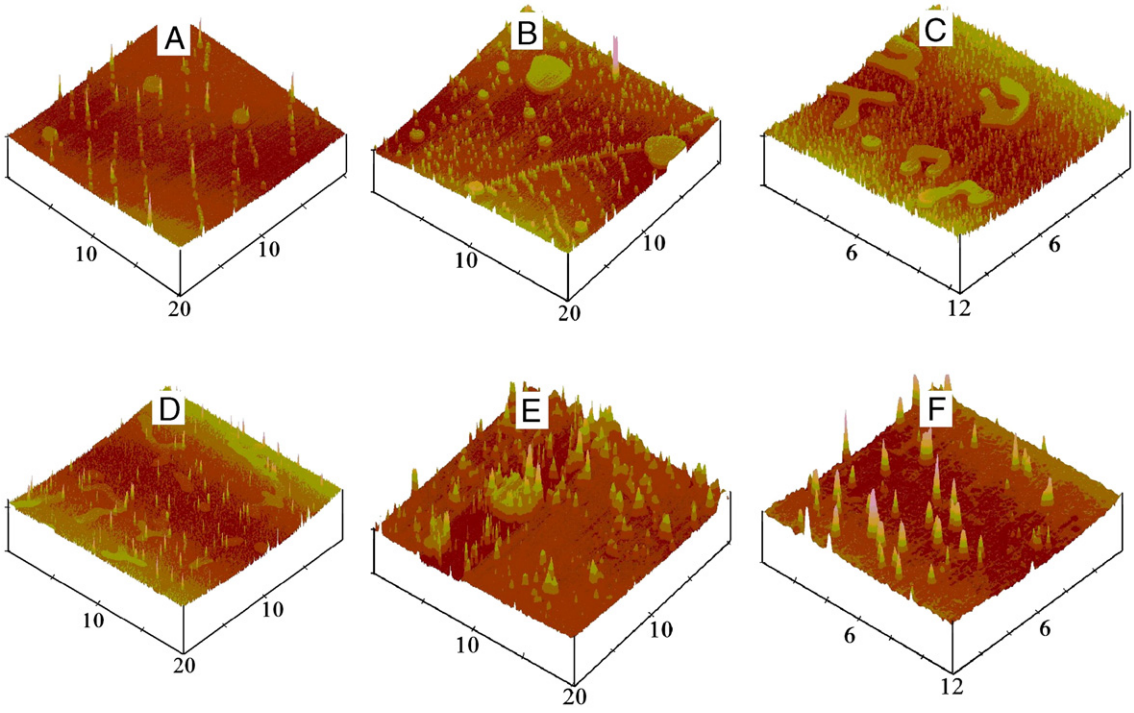

Fig. 6. Three dimensional view of the AFM images at different surface pressures (mN m^{-1}). A, 10; B, 20; C, 30; D, 40; E, 50 and F, 60. *X* (μm)–*Z* (nm) scales: A, B, C, E, F 20×5; D 12.5×5.

features of uneven patterns disappeared at $\pi > 60$ mN m^{-1}; the domains became smaller and nearly homogeneous. Usually, domain size increases with the π up to a certain extent, thereafter, with increasing π, surface active materials get dissolved into the subphase forming vesicles/aggregates with significant decrease in domain size at $\pi > 35$ mN m^{-1}. Similar trends were herein observed. We observed earlier [48] that at $\pi > 50$ mN m^{-1}, characteristic features of the surface disappeared due to the formation of multilayered structures at the interface. But unusual changes in shapes of the organized structures (domains) were herein observed. We presumed that it was due to i) lower cholesterol content, and ii) higher protein content in the GLSE. Low cholesterol content made the line tension across the domains uncontrollable to make the domain structures not restricted to the circular shape only. Similar results were also reported by others [54]. Utmost care was taken in this study to minimize the contamination of the LA fraction of PS, but protein content was found to be higher.

Surface heterogeneity was also examined for the three dimensional images of the LB deposits. Results are shown in Fig. 6. Small dots and lines observed in the diagrams were artifacts (dried

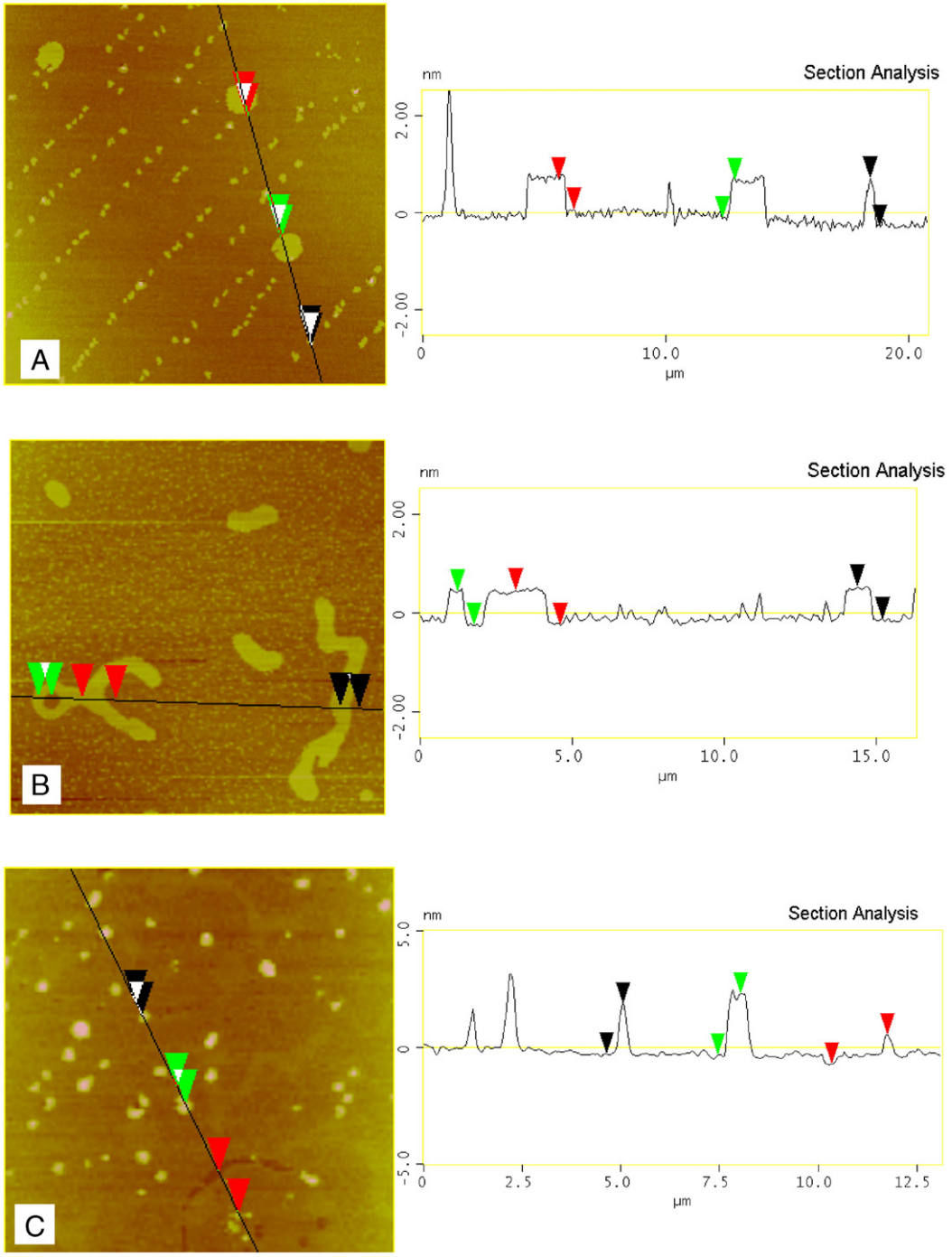

Fig. 7. Cross sectional analyses of GLSE films deposited on mica at different surface pressures (mN m^{-1}). A, 10; B, 30; and C, 60.

up salts contributed to it) in the subphase. Some non-specific proteins could have also contributed to the effect.

It is usually believed that the organized regions, (domains) are enriched with the saturated phospholipids DPPC, which is considered to remain more organized than its surroundings. Considering the cross sectional analyses, as shown in Fig. 7, the height differences between the domains and their surroundings were determined. A typical height difference of around 1.2 nm was expected from the AFM image analysis. Results are shown in the figure. The present system was a complex mixture of different phospholipids, simple lipids and proteins, and hence the height difference might not remain restricted within 1.2 nm. A height difference of around 0.8 nm was observed. This was in conformity with the results of other reported systems [39]. Even the elongated regions maintained the same height profile. At higher $\pi > 50$ mN m^{-1}, drastic change in the height profile was observed. The height difference between the organized regions and their surroundings was found to be ~0.8 nm at lower pressures which at higher pressures (>50 mN m^{-1}), was 2 nm on the average (Fig. 7). At high surface pressure, bovine lung surfactant is known to form stacked multilayers. The GLSE herein studied has been also considered to form multilayers. The observed elevation differences of around 2.0 nm were close to the value of a typical fluid monolayer [55] or alternately half the height of a bilayer. We, therefore, opine that at high surface pressure GLSE formed bilayers.

4. Conclusions

The PL content of GPS is comparable with mammalian PS; its protein content is not comparable with many whereas the CHOL content is smallest among all. The low percentage of CHOL has made the monolayer of GPS less rigid than other PS. ESIMS measurements have evidenced DPPC to be the major disaturated PL in GPS. The isolated GPS forms a monolayer at the air–water interface and undergoes two dimensional phase transitions, witnessed in π–A as well as C_S^{-1} (compressibility modulus)–A isotherms. The monolayer under compression forms domains of different categories. At moderate π, heterogeneous spherical domains are formed that get converted into noodle-like shapes on increasing $\pi \geq 30$ mN m^{-1}. Increased π converts them into heterogeneous domains with non-specific shapes. At higher pressure a part of the compressed GPS layer gets dissolved in the subphase to form vesicle-like aggregates; the interfacial material gets organized as stacks. The domain height at moderate pressure is 0.8 nm which is lower than the expected height of 1.2 nm; it increases to 2 nm at $\pi > 50$ mN m^{-1} by way of stacking of layers on the surface. The interfacial features of GPS compare well with that of other mammalian PS with differences here and there. The GPS thus has a prospect for use for the cure of respiratory distress syndrome both in infant and adult especially in India.

5. Unresolved issues and future projection

As per our literature survey, the present study is the first reasonably detailed investigation on GLSE. This initial study of the LA fraction of GLSE needs further exploration for its possible use as a potential clinical formulation in the Indian subcontinent as well as in the Asia Pacific region. To that end in view, further research on the exact composition of PS, quantification and characterization of two most important constituents SP-B and SP-C and determination of the functionality of GLSE is to be conducted. Additionally chemical compositions of the organized domains are to be ascertained with the help of techniques, Time of Flight Secondary Ionization Mass Spectrometry (TOFSIMS) and X-ray Photoelectron Spectroscopy (XPS).

Acknowledgements

Financial assistance from the Department of Science and Technology, Govt. of India, New Delhi in the form of a research grant is thankfully acknowledged. SM acknowledges the receipt of a JRF from the grant. KM thanks CSIR. SPM thanks INSA for an Honorary Scientist position. Authors also gratefully acknowledge the constructive suggestions made by both the reviewers.

References

[1] R.H. Notter, J.N. Finkelstein, Pulmonary surfactant: an interdisciplinary approach, J. Appl. Physiol.: Respir., Environ. Exercise Physiol. 57 (6) (1984) 1613–1624.
[2] R.E. Pattle, Properties, function and origin of the alveolar lining, Nature (London) 175 (1955) 1125–1126.
[3] J.A. Clements, Surface tension of lung extracts, Proc. Soc. Exp. Biol. Med. 95 (1957) 170–172.
[4] A.D. Bangham, Lung surfactant: how it does and does not work, Lung 165 (1987) 17–25.
[5] J. Goerke, Pulmonary surfactant: functions and molecular composition. Biochim. Biophys. Acta 1408 (1998) 79–89.
[6] J. Perez-Gil, K.M.W. Keough, Interfacial properties of surfactant proteins, Biochim. Biophys. Acta 1408 (1998) 203–217.
[7] F. Possmayer, Physicochemical aspects of pulmonary surfactant, in: R.A. Polin, W.W. Fox, S. Abman (Eds.), Fetal and Neonatal Physiology, 3rd ed., W.B. Saunders Company, Philadelphia, 2004, pp. 1014–1034.
[8] F. Possmayer, K. Nag, K. Rodriguez, R. Qanbar, S. Schürch, Surface activity in vitro; role of surfactant proteins, Comp. Biochem. Physiol., Part A Mol. Integer. Physiol. 129 (2001) 209–220.
[9] B. Piknova, V. Schram, S. Hall, Pulmonary surfactant: phase behaviour and function, Curr. Opin. Struck. Biol. 12 (2002) 487–494.
[10] R. Veldhuizen, K. Nag, S. Orgeig, F. Possmayer, The role of lipids in pulmonary surfactants, Biochim. Biophys. Acta 1408 (1998) 90–98.
[11] I. Freking, A. Gunther, W. Seeger, U. Pison, Pulmonary surfactant: functions, abnormalities and therapeutic options, Intensive Care Med. 27 (2001) 1699–1717.
[12] M. Griese, Pulmonary surfactant in health and human lung diseases: state of art, Eur. Respir. J. 13 (1999) 1455–1476.
[13] L.M.G. Van Golde, Potential role of surfactant proteins A and D in innate lung defense against pathogens, Biol. Neonate 67 (1995) 2–17.
[14] J. Floros, P. Kala, Surfactant proteins: molecular genetics of neonatal pulmonary diseases, Annu. Rev. Physiol. 60 (1998) 365–384.
[15] J.F. Lewis, R. Veldhuizen, Role of exogenous surfactant in the treatment of acute lung injury, Annu. Rev. Physiol. 65 (2003) 613–642.
[16] S.P. Yu, G.R. Harding, N. Smith, F. Possmayer, Bovine pulmonary surfactant: chemical composition and physical properties, Lipids 18 (1983) 522–529.
[17] R.H. Notter, S.A. Tabak, R.D. Mavis, Surface properties of binary mixtures of some pulmonary surfactant components, J. Lipid Res. 21 (1980) 10–12.
[18] J.G. Turcotte, A.M. Sacco, J.M. Steim, S.A. Tabak, R.H. Notter, Chemical synthesis and surface properties of an analog of the pulmonary surfactant dipalmitoylphosphatidylcholine, Biochim. Biophys. Acta 488 (1977) 235–248.

[19] J.C. Watkins, The surface properties of pure phospholipids in relation to those of lung extracts, Biochim. Biophys. Acta 152 (1968) 293–306.
[20] E.J.A. Veldhuizen, R.V. Diemel, G. Putz, et al., Effect of hydrophobic surfactant proteins on the surface activity of spread films in the captive bubble surfactometer, Chem. Phys. Lipids 110 (2001) 47–55.
[21] E.C. Crouch, Structure, biologic properties, and expression of surfactant protein D (SP-D), Biochim. Biophys. Acta 1408 (1998) 278–289.
[22] H.P. Haagsmab, R.V. Diemel, Surfactant associated proteins: functions and structural variations, Comp. Biochem. Physiol., Part A Mol. Integr. Physiol. 129 (2001) 91–108.
[23] S. Hagwood, M. Derrick, F. Poulain, Structure and properties of surfactant protein B, Biochim. Biophys. Acta. 1408 (1998) 150–160.
[24] J. Johansson, Structure and properties of surfactant protein C, Biochim. Biophys. Acta. 1408 (1998) 161–172.
[25] F.X. McCormack, Structure, processing and properties of surfactant protein A, Biochim. Biophys. Acta 1408 (1998) 109–131.
[26] T.E. Weaver, J.J. Conkright, Functions of surfactant proteins B and C, Annu. Rev. Physiol. 63 (2001) 555–578.
[27] B. Robertson, H.L. Halliday, Principles of surfactant replacement, Biochim. Biophys. Acta 1408 (1998) 346–361.
[28] J.Q. Ding, J.Y. Takamoto, A. von Nahmen, M.M. Lipp, K.Y.C. Lee, A.J. Warring, J.A. Zasadzinski, Effects of lung surfactant proteins, SP-B and SP-C, and palmitic acid on monolayer stability, Biophys. J. 80 (2001) 2262–2272.
[29] P. Kumar, P.S. Kiran, Changing trends in the management of Respiratory Distress Syndrome (RDS), Indian J. Pediatr. 71 (2004) 49–54.
[30] A.J. McCabe, D.T. Wilcox, B.A. Holm, P.L. Glick, Surfactant — a review for pedtriatic surgeons, J. Pediatr. Surg. 35 (2000) 1687–1700.
[31] R.H. Notter, Z. Wang, Pulmonary surfactant: physical chemistry, physiology and replacement, Rev. Chem. Eng. 13 (1997) 1–118.
[32] A.D. Bangham, C.J. Morley, M.C. Philips, The physical properties of an effective lung surfactant, Biochim. Biophys. Acta 573 (1979) 552–556.
[33] J.A. Clements, Functions of the alveolar lining, Am. Rev. Respir. Dis. 115 (1977) 67–71.
[34] T. Horie, J. Hildebrandt, Dynamic compliance, limit cycles and static equilibria of excised cat lung, J. Appl. Physiol. 31 (1971) 423–430.
[35] M. Gugliotti, M.J. Politi, The role of the gel/liquid-crystalline phase transition in the lung surfactant cycle, Biophys. Chemist. 89 (2001) 243–251.
[36] A. Engel, Y. Lyubchenko, D. Muller, Atomic force microscopy: a powerful tool to observe biomolecules at work, Cell Biol. 9 (1999) 77–90.
[37] L.F. Chi, M. Anders, H. Fuchs, R.R. Johnston, H. Ringsdorf, Domain structures in Langmuir–Blodgett films investigated by atomic force microscopy, Science 259 (1993) 213–216.
[38] C.W. McConlogue, T.K. Vanderlick, A close look at domain formation in DPPC monolayers, Langmuir 26 (13) (1997) 7158–7164.
[39] D.Y. Takamoto, M.M. Lipp, A. von Nahmen, K.Y. Lee, A.J. Warring, J.A. Zasadzinski, Interaction of lung surfactant proteins with anionic phospholipids, Biophys. J. 81 (2001) 153–169.
[40] A.K. Panda, K. Nag, R.R. Harbottle, K.R. Capote, R.A.W. Veldhuizen, N.O. Petersen, F. Possmayer, Effect of acute lung injury on structure and function of pulmonary surfactant films, Am. J. Respir. Cell Mol. Biol. 30 (2004) 641–650.
[41] E.G. Bligh, W.J. Dyer, A rapid method for total lipid extraction and purification, Can. J. Biochem. Physiol. 37 (1959) 911–913.
[42] Rouser, Phospholipid determination by phosphorous assay, Lipids 5 (1976) 494–496.
[43] J.T. Ireland, The calorimetric estimation of total cholesterol in whole blood, serum, plasma and other biological material, Biochem. 35 (1941) 283–293.
[44] O. Folin, V. Ciocalteu, On tyrosine and tryptophane determinations in proteins, J. Biol. Chem. 73 (1927) 627–650.
[45] O.H. Lowry, N.J. Rosebrough, A.L. Farr, R.J. Randall, Protein measurement with the Folin phenol reagent, J. Biol. Chem. 193 (1951) 265–275.
[46] C.J. Lang, A.D. Postle, S. Orgeig, F. Possmayer, W. Bernhard, A.K. Panda, K.D. Jurgens, W.K. Milsom, K. Nag, C.B. Daniels, Dipalmitoylphosphatidylcholine is not the major surfactant phospholipid species in all mammals, Am. J. Physiol., Regul. Integr. Comp. Physiol. 289 (2005) 1426–1439.
[47] A.D. Postle, A. Mander, K.B.M. Reid, J.Y. Wang, S.M. Right, M. Moustaki, J.O. Warner, Deficient hydrophilic lung surfactant proteins A and D with normal surfactant phospholipid. Molecular species in cystic fibrosis, Am. J. Respir. Cell Mol. Biol. 20 (1999) 90–97.
[48] K. Nag, M. Fritzen-Garcia, R. Devraj, A.K. Panda, Interfacial organizations of gel phospholipid and cholesterol in bovine lung surfactant films, Langmuir 23 (2007) 4421–4431.
[49] Z. Wang, S.B. Hall, R.H. Notter, Dynamic surface activity of films of lung surfactant phospholipids, hydrophobic proteins, and neutral lipids, J. Lipid Res. 36 (1995) 1283–1293.
[50] K. Nag, J. Perez-Gill, M.L.F. Ruano, L.A.D. Worthman, J. Stewart, C. Casals, K.M.W. Keough, Phase transitions of the films of lung surfactants at the air–water interface, Biophys. J. 74 (1998) 2983–2995.
[51] B.M. Discher, K.M. Maloney, W.R. Scheif, D.W. Grainger, V. Vogel, S.B. Hall, Lateral phase separation in interfacial films of pulmonary surfactants, Biophys. J. 71 (1996) 2583–2590.
[52] S. Schürch, R. Qanbar, H. Bacofen, F. Possmayer, The surface associated surfactant reservoir in the alveolar lining, Biol. Neonate 67 (1995) 61–76.
[53] S. Schürch, F.H.Y. Green, H. Bacofen, Formation and structure of surface films: captive bubble surfactometry, Biochim. Biophys. Acta 1408 (1998) 180–202.
[54] P. Kruger, M. Losche, Molecular chirality and domain shapes in lipid monolayers on aqueous surfaces, Am. Phys. Soc. (2000) 7031–7043.
[55] J. Lauger, C.R. Robertson, C.W. Frank, G.G. Fuller, Deformation and relaxation processes of mono- and bilayer domains of liquid crystalline Langmuir films on water, Langmuir 12 (23) (1996) 5630–5635.
[56] N.J. Foot, S. Orgeig, C.B. Daniels, The evolution of a physiological system: the pulmonary surfactant system in diving mammals, Respir. Physiol. Neurobiol. 156 (2006) 118–138.
[57] G.A. Rau, G. Vieten, J.J. Haitsma, J. Freihorst, C. poets, B. M Ure, W. Bernharad, Surfactant in newborn compared with adolescent pigs, adaptation to neonatal respiration, Am. J. Respir. Cell Mol. Biol. 30 (2004) 694–701.
[58] A.D. Postle, E.L. Heeley, D.C. Wilton, A comparison of the molecular species compositions of mammalian lung surfactant phospholipids, Comp. Biochem. Physiol., Part A 129 (2001) 65–73.